



Correction of the Observatoire Haute Provence electrochemical concentration cell (ECC) ozonesonde 1991-2023 data record

Sachiko Okamoto^{1,2}, Gérard Ancellet¹, Sophie Godin-Beekmann¹, and Renaud Bodichon³

¹LATMOS, Sorbonne Université, Université Versailles St-Quentin, CNRS/INSU, Paris, France

²now at: National Institute for Environmental Studies, Tsukuba, 350-8506, Japan

³IPSL, Sorbonne Université, Université Versailles St-Quentin, CNRS/INSU, Paris, France

Correspondence: Sachiko Okamoto (okamoto.sachiko@nies.go.jp) and Gérard Ancellet (gerard.ancellet@latmos.ipsl.fr)

Abstract. The Observatoire Haute Provence (OHP) station is one of the few long-term measuring stations for vertical ozone profiles in southern Europe. Since 1991, vertical ozone distribution has been monitored by the OHP weekly electrochemical concentration cell (ECC) ozonesonde. In this study, we have corrected the ECC datasets for the period 2002–2007. The correction of the ECC has been carried out using comparisons with other ozone-measuring instrument at the same station, stratospheric lidar, and with collocated satellite observations of the ozone vertical profile by Microwave Limb Sounder (MLS). Median ozone concentration of the ECC for the period 2002–2007 was -3.4 % lower than that of the stratospheric lidar and MLS. The ECC internal pump temperature showed a sudden drop of 16 K at 25 km for the period 2002–2007 compared to the period 1991–2001. Considering the long-term trends of the ECC current and stratospheric lidar ozone concentration at 25 km as well as the ECC pump speed trend, we show that the observed ECC pump temperature between 2002 and 2007 is too low by -10 K at 25 km. The ECC pump temperature for the period 2002–2007 has been corrected accordingly by 0 K at 0 km and 10 K at 30 km and the bias at 25 km with the stratospheric lidar and MLS have been reduced to -0.5 %.

1 Introduction

The stratospheric ozone layer recovery is expected considering the decrease of the ozone-depleting substances (ODSs) because of the Montreal Protocol and its amendments (WMO, 2023). In the upper-stratosphere (above 35 km), ozone increase has been confirmed by various studies e.g. (Godin-Beekmann et al., 2022; Petropavlovskikh et al., 2025; Steinbrecht et al., 2017). The monitoring of ozone in the upper troposphere and lower stratosphere (UTLS) region is crucial for Earth's radiation budget e.g. (Riese et al., 2012) and for modulating air quality near Earth's surface via deep stratospheric intrusions e.g. (Lin et al., 2015). Despite its importance, the confidence in the long-term ozone trends in the UTLS remains low (Godin-Beekmann et al., 2022; Petropavlovskikh et al., 2025; Steinbrecht et al., 2017; Van Malderen et al., 2021). The longest records of the vertical ozone distribution in the stratosphere are provided by balloon borne ozonesondes regularly launched at more than 50 stations around the world. The ozonesonde is a small and lightweight instrument that measures atmospheric ozone profiles up to about 30–35 km (Komhyr, 1969; Komhyr et al., 1995). The ozone measurement is based on the electrochemical method where ozone is titrated in a potassium iodide (KI) sensing solution. The chemical transformation generates an electric current proportional to the amount of ozone; hence the name electrochemical concentration cell (ECC). Data of many ozonesonde stations were



25 recently reprocessed to reduce uncertainties in ozone trends (Ancellet et al., 2022; Sterling et al., 2018; Tarasick et al., 2016; Van Malderen et al., 2016; Witte et al., 2017, 2018), but some instrumental artifacts still need to be addressed at some stations (Smit and Thompson, 2021). The homogenization of the ozonesonde records followed the Ozonesonde Data Quality Assessment (O3S-DQA) panel recommendations (Smit et al., 2012). At the Observatoire de Haute Provence (OHP: 43.93° N, 5.71° E), ozone vertical profile monitoring has been carried out since the mid-1980s by ozonesondes and lidar observations. The
30 OHP is one of the few long-term measuring stations for vertical ozone profiles in Southern Europe. Improvement and homogenization of the ECC ozone observations at OHP from 1991 to 2021 has been detailed in Ancellet et al. (2022). However ECC total columns after homogenization still show underestimated values for the 2005-2007 period when looking at comparisons with satellite observations (Fig. 9 in Ancellet et al. (2022)). Therefore detailed comparisons of OHP ECC profiles with lidar and Microwave Limb Sounder (MLS) observations are needed in the stratosphere. This paper begins with an overview of the
35 ozonesonde measurement system, and brief descriptions of stratospheric lidar and the MLS data in section 2 followed by a comparison of ozone concentrations between ozonesonde and collocated lidar/MLS records in section 3. The reprocessing approach and methodology are described in section 4. The analyses that compare the original and reprocessed time series are also described. The conclusion appears in section 5.

2 Data

40 2.1 Ozonesonde

The ECC ozonesondes have been used since 1991 to measure ozone vertical profile every week (generally around 09:00 UT). The ECC generates an electrical current through the reaction of ozone in a KI solution. The ozone partial pressure P_{O_3} (measured in mPa) is then obtained from the electrochemical current I_M (measured in μA), the background current I_B measured in the preparation laboratory with an ozone removal filter after the sonde was exposed to ozone, the gas volume flow
45 rate Φ_P (in $cm^3 \cdot s^{-1}$) of the air sampling pump, its temperature T_P (in K) and the total efficiency of the ozone sensor η_T (Smit and Thompson, 2021).

$$P_{O_3} = \frac{4.306 \cdot 10^{-2} \cdot T_P}{\eta_P \cdot \eta_A \cdot \eta_C \cdot \Phi_P} \cdot (I - I_b) \quad (1)$$

The total efficiency η_T consists of pump flow efficiency η_p , absorption efficiency η_A and conversion efficiency of the absorbed ozone η_C . The median value of the relative uncertainty in the ozone concentration measured by the ECC is on the order of
50 6–7 % in the stratosphere (Ancellet et al., 2022). Total column ozone (TCO) measurements by the UV-visible SAOZ (Système d'Analyse par Observation Zénithale) and the Dobson spectrophotometer are available at OHP. The so-called normalization factor is calculated as the ratio of the spectrophotometer TCO and the ECC TCO. Historically, ozonesonde profiles have often been normalized or scaled to an independent measurement of the TCO. Normalization of ECC sonde profiles is no longer recommended, however the normalization factor provides a useful indicator for the quality of ozonesonde profile data and the
55 consistency in ozonesonde data time series. We use the dataset of the Dobson spectrophotometer from 1991 to 2004 and of the



SAOZ from 2004 to 2023 to calculate normalization factor. Only ozonesonde profiles with a normalization factor below 1.3 are considered here.

The details of instrument changes and the homogenization are described in Ancellet et al. (2022). Briefly, the main changes considered in this work are as the following: a major change in the sounding procedure occurred in March 1997 when the Science Pump Corporation (SPC) ozonesonde was replaced by the Environmental Science Corporation (EnSci) ozonesonde. In July 2007, the radiosonde type switched from Vaisala RS80 to MODEM M10, together with a change of the position of pump temperature inserted in the pump hole instead of being taped to the pump. No significant sounding preparation occurred during the time period March 1997 and July 2007. Correction of T_p has been implemented to account for the changes in the position of the ECC pump thermistor in June 2007. However the ECC pump temperature record remains inhomogeneous for the the period 1991-June 2007 and this correction must be carefully assessed. In this work, the ECC pump temperature correction is assessed by comparison of corrected ECC ozone concentrations with other ozone measurements obtained at OHP in as close coincidence as possible.

2.2 Lidar

At OHP, regular nighttime measurements (2–4 per week) by the Differential Absorption Lidar (DIAL) ozone lidar have been made since 1985 (Godin-Beekmann et al., 2002). The lidar is optimized for stratospheric ozone profiling between 10 and 50 km a.s.l. using an absorbed wavelength at 308 nm and a reference wavelength at 355 nm. Ozone profiles are obtained during the night in clear sky conditions and over a time range of 4 hours. The best accuracy (5 %) is generally obtained in the 15–40 km altitude range when ozone concentrations are large enough to minimize lidar systematic errors and signal-to-noise ratio (SNR) is maximum (Nair et al., 2011; Wing et al., 2020). The coincidence is determined with a temporal criterion of ± 12 h of the ECC sonde launch time for the comparison.

2.3 MLS

The Microwave Limb Sounder (MLS) on-board the Aura satellite measures vertical profiles of the abundances of key atmospheric species, including ozone. We use Aura MLS version 5.0x ozone volume-mixing ratio vertical profile observations (Schwartz et al., 2020) for a comparison with the ECC ozonesonde time series. The accuracy from 68 hPa to 4.6 hPa is 5–8 % (Livesey et al., 2022). The coincidence with the ECC sonde launch is determined with spatial differences less than $\pm 2.5^\circ$ latitude and $\pm 8^\circ$ longitude, and temporal differences less than ± 12 h. Using a smaller domain would significantly decrease the number of coincidences. Data screening based on the recommended values of the status flag, quality field and convergence field have been applied to the MLS data selected for the analysis of the stratospheric ozone profiles above OHP.

3 Comparison of ECC ozone concentrations with MLS and lidar

The monthly mean ozone concentrations of the ECC ozonesonde and the stratospheric lidar are compared for a layer of 2 km thickness at 25 km (Fig. 1a). Monthly mean differences between ECC and lidar ozone concentrations are shown in Fig. 1c



with frequent occurrences of negative differences before 2007. The median relative difference is -4.6% for the period January 2002–June 2007, while the mean relative differences are -3.3% and -0.3% for the period March 1997–December 2001 and July 2007–December 2023, respectively (Fig. 1c). Considering coincident measurements within ± 12 h, the difference between the ECC ozonesonde and the lidar for the period January 2002–June 2007 can be reduced (Fig. 1b and d). The median relative difference is nevertheless as large as -3.4% for the period January 2002–June 2007, while the mean relative differences are -2.0% and 0.1% for the period March 1997–December 2001 and July 2007–December 2023, respectively (Fig. 1d). The two times standard error on the median value is less than 1.5% . So the bias is still significant for the period January 2002–June 2007.

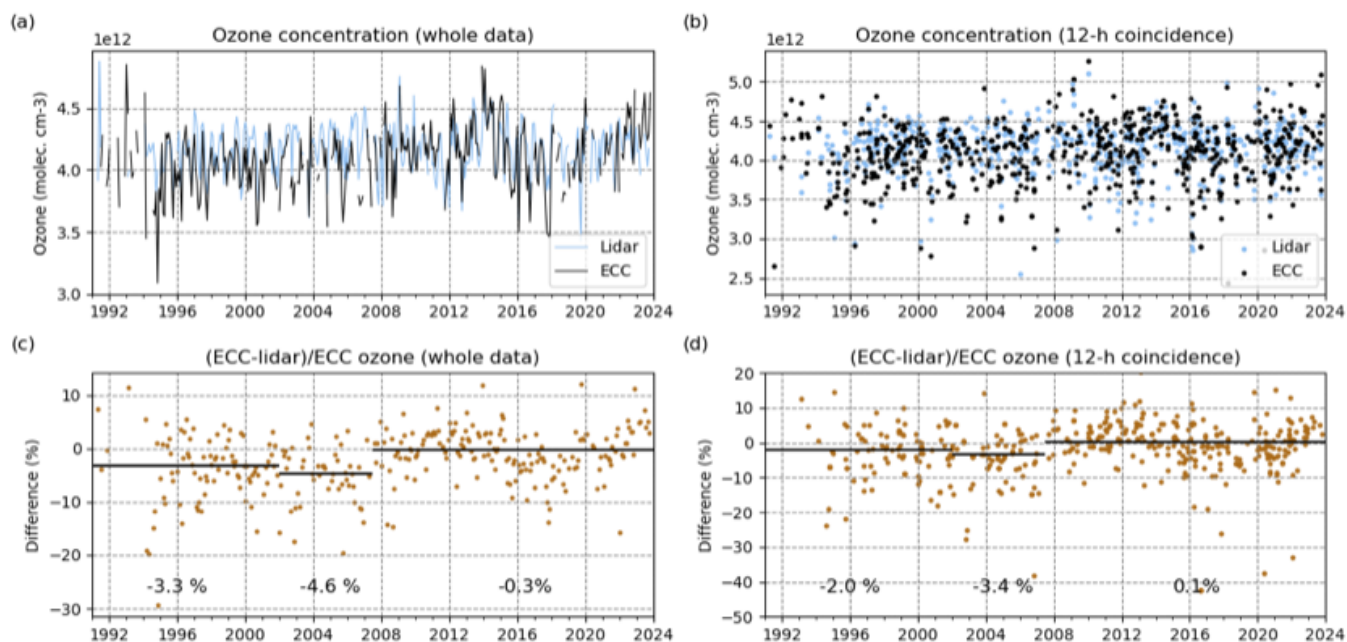


Figure 1. Time series of the ozone concentration of the stratospheric lidar and the ECC ozonesonde at 25 km. Ozone concentrations are calculated at altitude 25 km by averaging ozone over a range of ± 1 km. (a) Monthly mean and (c) mean relative ECC minus lidar ozone concentration differences (in %). Monthly means are calculated for the months which the number of observations in each month is greater than or equal to 3. (b) Ozone concentration and (d) relative ECC minus lidar ozone concentration differences for the coincident (< 12 h) profiles. Black lines with values in (b) and (d) indicate median relative differences for three periods: January 1991–December 2001, January 2002–June 2007 and July 2007–December 2023.



95 We have also compared ozone concentrations between the ECC ozonesonde and MLS at 26.1 hPa for the period January
2005–December 2023 (Fig. 2). The median relative difference for the period January 2005–June 2007 is also -3.4% which is
larger than that for the period July 2007–December 2023 (Fig. 2b). The two times standard error on the median value being
now as large as 4.0% . So the bias is not very significant when considering MLS for the period January 2002–June 2007.
Nevertheless the sign of the bias is similar to the results obtained when comparing ECC and lidar for the period 2002–2007.
100 Therefore, we investigated the cause of the underestimation based on Eq. 1 and the statistical distributions of the parameters
used to calculate the partial pressure of ozone.

4 Results and discussion

4.1 Time evolution of ozonesonde pump temperature

ECC internal pump temperature correction is one of the key factors in calculating ozone partial pressure as shown in section
105 2.1. Figure 3 shows its time evolution with three periods showing changes in the range of the ECC pump temperature. Values
are in the range 300–310 K after July 2007 while they are in the range 290–300 K before January 2002. This could be explained
by a major change of the ECC installation in the Styrofoam box when switching from Vaisala RS80 to MODEM M10 (new
electronic interface and new batteries). However the pump temperature has often dropped in the range 280–290 K between
January 2002 and July 2007 without a clear explanation for such a negative drop. Eventhough the homogenization in Ancellet
110 et al. (2022) accounted for the temperature positive correction due to the position of the thermistor being taped instead of
being inserted in the pump hole before July 2007. The unusually low values of the ECC pump temperature in 2002–June 2007
corresponds to that of the ozone concentration observed in section 3. A correction of the ECC pump temperature measurement
for this time period is then needed. Other factors, namely, ozone concentration change in the stratosphere and the statistical
distribution of the pump flow rate or the ECC current must be taken into account before we apply such correction.

115 To verify the effect of the ECC temperature drop for the period January 2002–June 2007 on the ECC ozone concentration at
25 km, the measured ECC temperature drop has been compared with a ECC temperature drop calculated by using measured
ECC current, pump flow and ozone concentration based on the Eq. (1). The ozone concentration measured by the stratospheric
lidar at OHP is employed assuming that it is the best proxy to account for any long term ozone change in the stratosphere. We
consider three periods: March 1997–December 2001 as period 1, January 2002–June 2007 as period 2 and July 2007–December
120 2023 as period 3 in this analysis. We did not use the data before March 1997 to avoid considering a change of the efficiency
of the ozone sensor η_T when changing the type of ozonesonde in March 1997. The distributions and medians of the ECC
temperature, the ECC current, the pump flow and the ozone concentration of lidar are shown in Fig. 4 and Table 1. The
differences of ozone concentration observed by lidar among three periods are small ($0-1\%$).

The calculated percentage difference of ECC temperature derived from observed differences of ECC current and pump flow
125 rate can be expressed as:

$$\frac{\Delta T_P}{T_P} = \frac{\Delta O_3}{O_3} - \frac{\Delta(I_M - I_B)}{(I_M - I_B)} - \frac{\Delta(1/\Phi_P)}{(1/\Phi_P)} \quad (2)$$

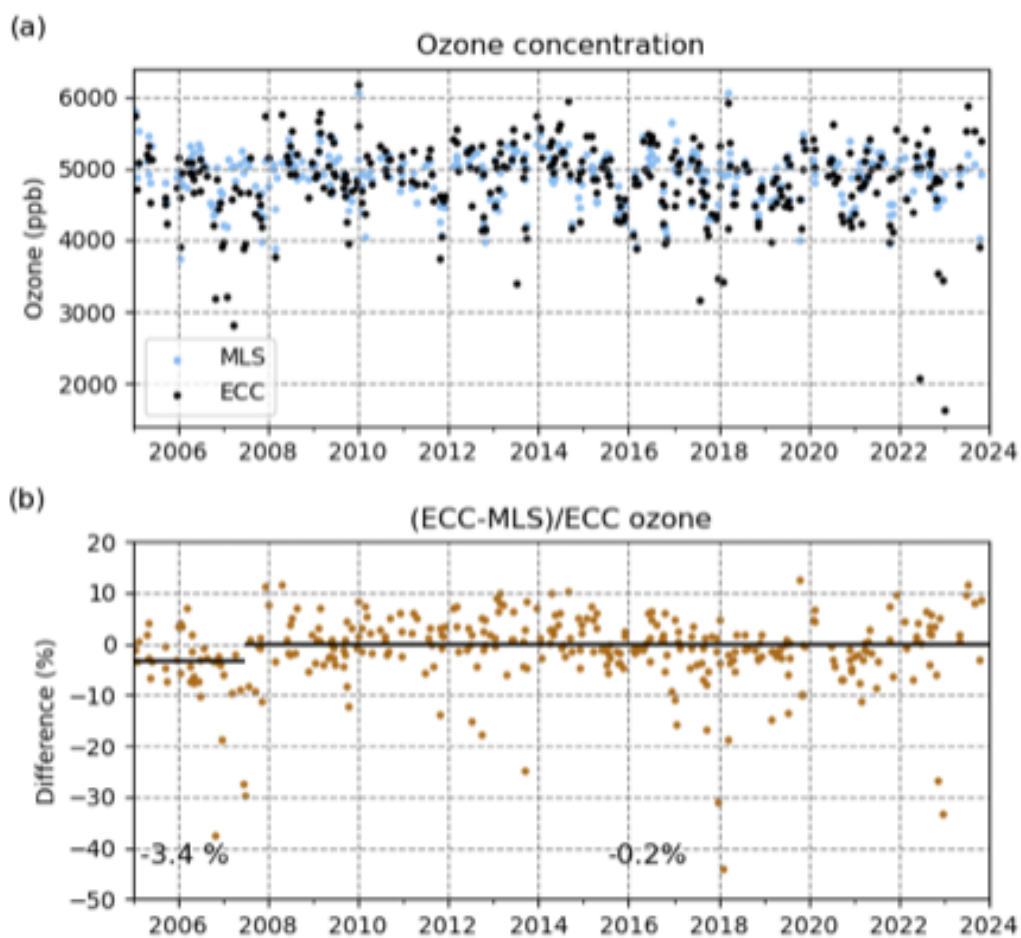


Figure 2. Time series of the ozone concentration of MLS and the ECC ozonesonde at 25 km. Ozone concentrations are calculated at pressure level 26.1 hPa by averaging ozone over a range of ± 1 km layer (31.6 hPa–21.5 hPa). (a) Ozone concentration and (c) relative ECC minus MLS ozone concentration differences (in %) for the coincident (< 12 h) profiles. Black lines with values in (b and d) indicate median relative differences for three periods: January 1991–December 2001, January 2002–June 2007 and July 2007–December 2023.

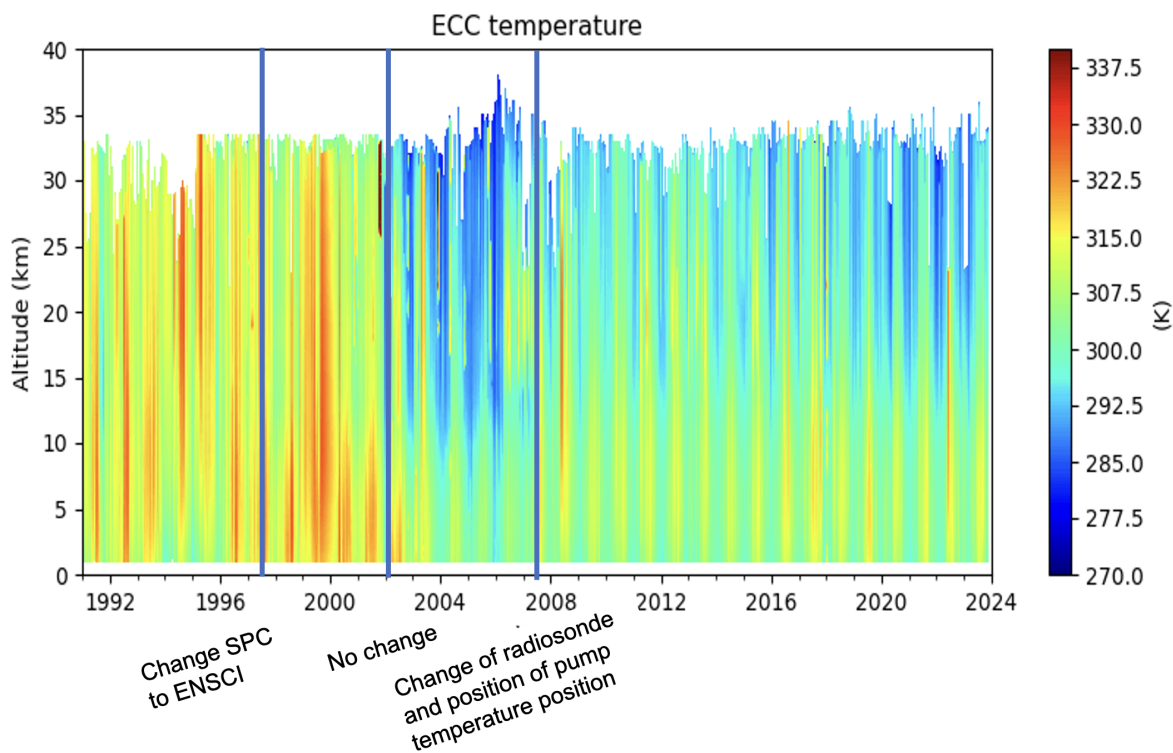


Figure 3. Time evolution of the ozonesonde internal pump temperature as a function of altitude. Major changes of the ECC instrument are shown in the bottom part of the figure.

Table 1. Medians of measured the ECC temperature, the current, the pump flow and the ozone concentration measured by the stratospheric lidar for three periods: March 1997–December 2001, January 2002–June 2007 and July 2007–December 2023.

	Period 1	Period 2	Period 3
Pump Temperature T_p	306.06 K	289.84 K	294.71 K
Current $I_M - I_B$	3.38 μA	3.58 μA	3.47 μA
Pump Flow $1/\Phi_p$	28.55 s	27.84 s	29.52 s
O₃ concentration in molecule.cm⁻³	4.18 10^{12}	4.22 10^{12}	4.22 10^{12}

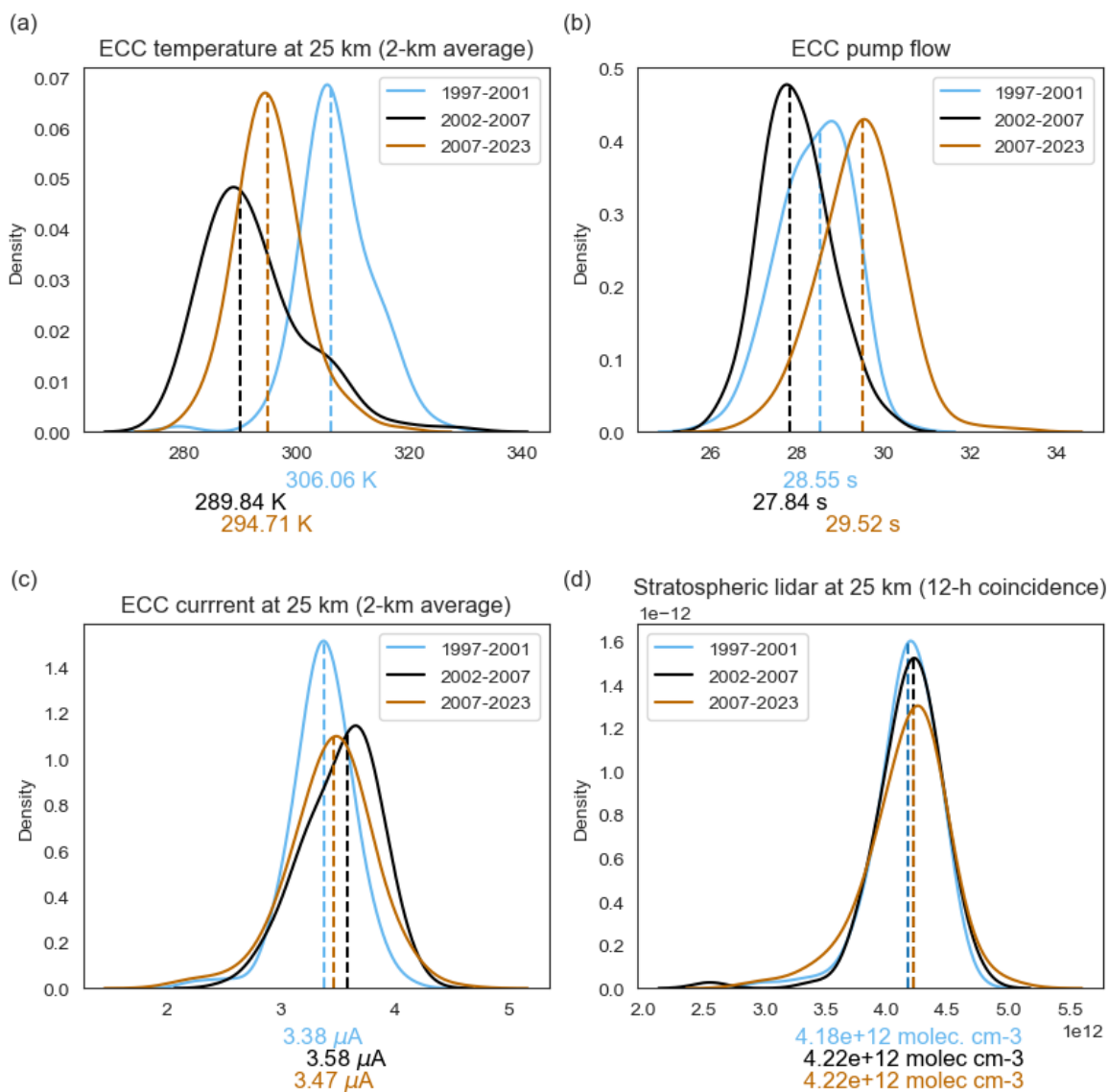


Figure 4. Density plot of the key factors in calculating the ozone partial pressure. (a) ECC temperature at 25 km, (b) ECC pump flow, (c) ECC current at 25 km, and (d) ozone concentration measured by the stratospheric lidar at OHP for three periods: March 1997–December 2001 (light blue), January 2002–June 2007 (black) and July 2007–December 2023 (brown). The dashed lines and values in the bottom part of figures show medians summarized in Table 1.



Table 2. Differences of calculated pump Temperature ΔT_{Pc} using differences of measured current $\Delta(I_M - I_B)$, pump flow $\Delta 1/\Phi$ and ozone concentration by lidar ΔO_3 for three periods: March 1997–December 2001, January 2002–June 2007 and July 2007–December 2023. The calculated pump Temperature difference ΔT_{Pc} is compared with the measured pump Temperature difference ΔT_P .

	Period 2 - Period 1	Period 3 - Period 1
$\Delta O_3/O_3$	1.0 %	1.0 %
$\Delta(I_M - I_B)/(I_M - I_B)$	5.75 %	2.63 %
$\Delta(1/\Phi_P)/(1\Phi_P)$	-2.52 %	3.34 %
$\Delta T_{Pc}/T_{Pc}$	-2.23 %	-5.0 %
ΔT_{Pc}	-6.6 K	-15.0 K
ΔT_P	-16.2 K	-11.4 K
$\Delta T_P - \Delta T_{Pc}$	-9.6 K	-3.6 K

Percentage differences are shown in Table 2 using measured values of period 2 and 3, i.e. when ozone underestimate change from -3.4 % to 0.1 %. Taken period 1 as a reference, measured and calculated differences are not significantly different for period 3 (< 4K) while their difference can be as large as -10 K for period 2.

130 4.2 ECC pump temperature correction

An ECC pump temperature correction was therefore applied for the period January 2002–June 2007 by increasing the ECC pump temperature linearly with altitude. Since according to section 4.1, bias of the ECC pump temperature can be as large as -10K in period 2 above 25 km, corrected ECC temperature T_{Pcor} is calculated as:

$$T_{Pcor} = T_P + \alpha z \quad (3)$$

135 where z is altitude (measured in km). We test three cases: $\alpha = 0.17$ ($\Delta T_P = 0$ K at 0 km and $\Delta T_P = 5$ K at 30 km) called version 2, $\alpha = 0.33$ ($\Delta T_P = 0$ K at 0 km and $\Delta T_P = 10$ K at 30 km) called version 3 and $\alpha = 0.50$ ($\Delta T_P = 0$ K at 0 km and $\Delta T_P = 15$ K at 30 km) called version 4 in addition to $\alpha = 0$ which is the uncorrected ECC temperature case. Four time evolutions of ECC temperature are displayed in Fig. 5. We can see that the observed drop of ECC temperature for the period January 2002–June 2007 is improved in version 3 and version 4.

140 To compare with the ozone concentrations of the stratospheric lidar and MLS, ozone concentrations are calculated by using three corrected ECC temperatures. Originally, median ozone concentration of the ozonesonde at 25 km for period 2 shows -3.4 % lower compared with those of the lidar and MLS (Fig. 1d and 2b). Ozone concentration corrected by the ECC temperature version 2 is still -2.0 % lower (Fig 6). The ECC correction version 3 ($\Delta T_P = 0$ K at 0 km and $\Delta T_P = 10$ K at 30 km) should reproduce ozone concentration which is equivalent to that of the stratospheric lidar according to Table 2. The ECC median
 145 ozone concentration corrected by the ECC temperature version 3 is -0.5 % lower than the lidar median ozone concentration during the period 2 (January 2002–June 2007). This -0.5 % bias lies between the median difference obtained during period 3

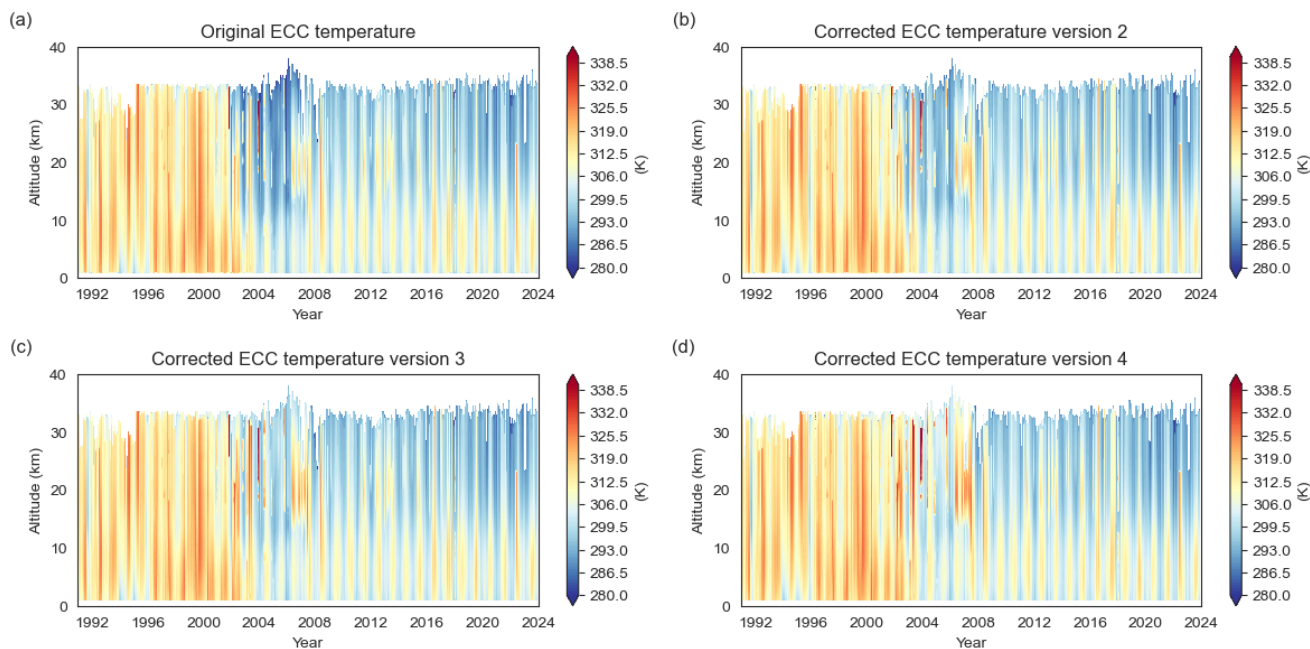


Figure 5. Time evolutions of ozonesonde pump temperature as a function of altitude. (a) Original ECC temperature is corrected by using the value (b) $\alpha = 0.17$, (c) $\alpha = 0.33$ and (d) $\alpha = 0.50$ in Eq. (3) for the period January 2002–June 2007.

(0.1 %) and during period 1 (-2 %). Comparisons between the ozonesonde and MLS show similar improvement of the bias with insignificant differences for version 3 and 4 considering the large standard errors.

Normalization factor is also a useful indicator for the consistency in ozonesonde data time series. The normalization factor corrected by the ECC temperature version 4 is unable to maintain a stationary time evolution of the normalization factor from 1991 to 2024 since a well defined drop of the of the normalization factor occurs during the 2002-June 2007 period (Fig. 7d). The result supports that the correction by the ECC temperature version 3 is the best option to improve the current homogenization work of the OHP ECC time series from January 2002 to June 2007.

The ozone concentrations of the ECC ozonesonde version 3 are compared to the stratospheric lidar for a layer of 2 km thickness at 25 km in figure 8a-b. The corresponding ECC data can be accessed at repository under data DOI (Ancellet and Godin-Beekmann, 2025). The correction by the ECC temperature improves the difference from -3.4 % to -0.5 %. The correction only slightly improves the median difference between the ECC ozonesonde and MLS at 26.1 hPa from -0.5 % to -0.2 % (Fig. 8c-d).

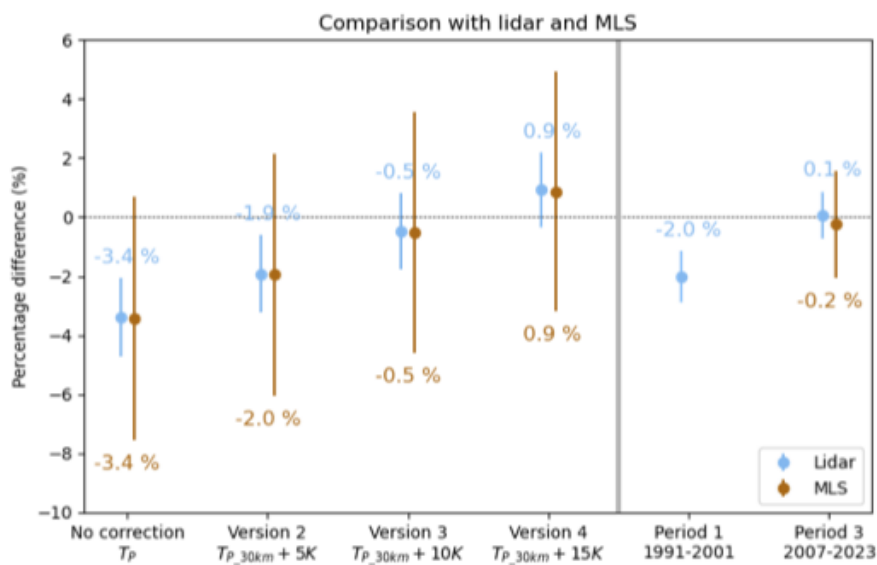


Figure 6. Evaluation of ECC ozone concentration compared with lidar and MLS ozone concentrations. Results are presented as medians and 2*standard errors of percentage difference for a corrected and two uncorrected periods. An uncorrected and three corrected ECC ozone concentrations are tested for the period January 2002–June 2007.

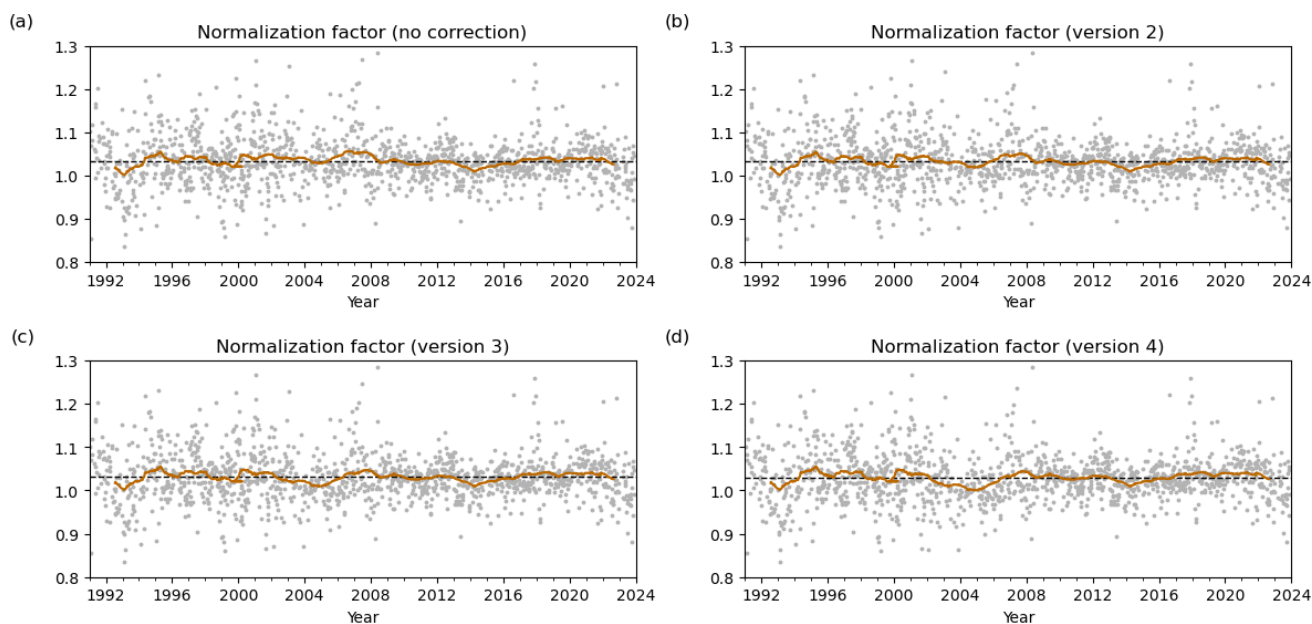


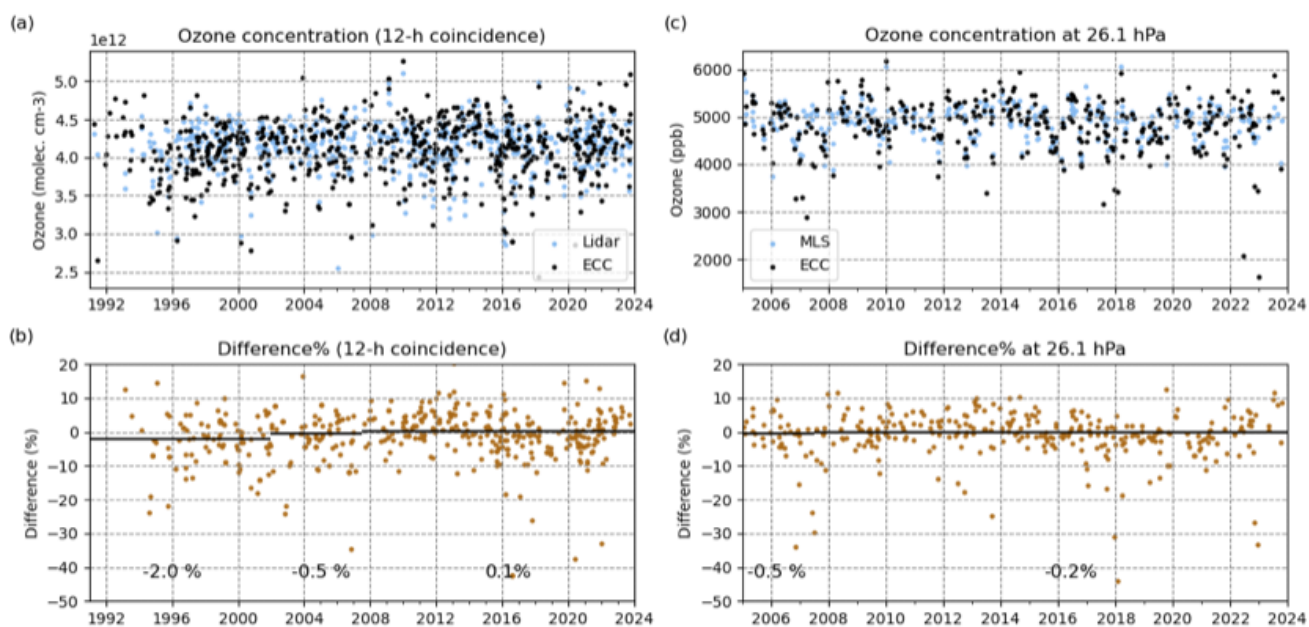
Figure 7. Time evolution of the ECC normalization factor. The dashed black lines are averages of normalization factors for the period January 1991–December 2023. The thick brown lines are the 100-point, centered, moving averages.

5 Conclusions

160 The ozonesonde dataset at OHP has been corrected based on an analysis of the ECC internal pump temperature for the period
January 2002–June 2007. Despite the dataset homogenization for the period 1991–2021 according to the recommendations of
the O3S-DQA (Smit and Thompson, 2021; Ancellet et al., 2022), we found that mean ozone concentration of the ECC for the
period 2002–2007 was -3.4 % lower than that of the stratospheric lidar at the same station and collocated satellite observations
by MLS. The ECC pump temperature showed a sudden drop of 16 K at 25 km for the period 2002–2007 compared to the
165 period 1991–2001. Taken the 1991–2001 period as a reference, observed ECC temperature decrease for the period after June
2007 is consistent with changes of the other measured parameters (flow rate, ECC current). However the -16.6 K temperature
decrease during the period 2002–2007 is too large and must be corrected by almost 10 K to match changes of the other measured
parameters. The ECC pump temperature for the period January 2002 – June 2007 has been corrected accordingly by 0 K at 0
km and 10 K at 30 km and the bias at 25 km with the stratospheric lidar and MLS have been reduced to -0.5 %.

170 6 Code and data availability

The uncorrected OHP ECC data are available at <https://doi.org/10.25326/293>. The corrected OHP ECC data are available at
<https://dx.doi.org/10.25326/855> (Ancellet and Godin-Beekmann, 2025).



1

Figure 8. Time series of ozone concentration of the stratospheric lidar and the ECC ozonesonde at 25 km, and MLS and the ECC ozonesonde at 26.1 hPa. (a and c) Ozone concentration and (b and d) relative ECC minus lidar ozone concentration differences for the coincident (< 12 h) profiles. Ozone concentrations for (a–b) are calculated at altitude 25 km by averaging ozone over a range of ± 1 km. Ozone concentrations for (c–d) are calculated at pressure level 26.1 hPa by averaging ozone over a range of ± 1 layer (31.6 hPa–21.5 hPa). Black lines with values in (b and d) indicate average relative differences for the periods same as Fig. 1-2.



The OHP Stratospheric DIAL data are available at <https://www-air.larc.nasa.gov/missions/ndacc/data.html?station=haute-provence/ames/lidar/>

175 The MLS stratospheric ozone data are available at the NASA Goddard Space Flight Center Earth Sciences Data and Information Services Center (GES DISC): https://disc.gsfc.nasa.gov/datasets/ML2O3_005/summary (Schwartz et al., 2020).

The OHP ECC homogenization code is available on request from Renaud Bodichon (renaud.bodichon@ipsl.fr)

180 *Author contributions.* G. Ancellet (GA) and S. Godin-Beekmann (SGB) designed the work plan and are the PI of the OHP ozone ECC and lidar instruments. Sachiko Okamoto (SO) carried out the work and wrote the manuscript. Renaud Bodichon (RB) manages the data sets and the ECC processing codes

Competing interests. No competing interest are present

Acknowledgements. The work was supported by the French National Research Agency via the ALPHA-O3 Projet-ANR-22-CE01-0007 <https://anr.fr/Projet-ANR-22-CE01-0007>

185 The authors acknowledge the AERIS and NDACC data infrastructures for hosting the OHP data base. The technical staff of the Observatoire de Haute Provence are gratefully acknowledged for carrying out the ECC ozone soundings and the stratospheric lidar measurements.

The MLS data processing team is gratefully acknowledged for providing the satellite data.



References

- Ancellet, G., Godin-Beekmann, S., 2025. O₃ profiles data using 2025-corrected ECC ozonesonde measurements at OHP. ACTRIS Dataset. URL: <https://dx.doi.org/10.25326/855>, doi:<https://doi.org/10.25326/855>.
- 190 Ancellet, G., Godin-Beekmann, S., Smit, H.G.J., Stauffer, R.M., Van Malderen, R., Bodichon, R., Pazmiño, A., 2022. Homogenization of the observatoire de haute provence electrochemical concentration cell (ecc) ozonesonde data record: comparison with lidar and satellite observations. *Atmospheric Measurement Techniques* 15, 3105–3120. URL: <https://amt.copernicus.org/articles/15/3105/2022/>, doi:<https://doi.org/10.5194/amt-15-3105-2022>.
- Godin-Beekmann, S., Azouz, N., Sofieva, V.F., Hubert, D., Petropavlovskikh, I., Effertz, P., Ancellet, G., Degenstein, D.A., Zawada, D., Froidevaux, L., Frith, S., Wild, J., Davis, S., Steinbrecht, W., Leblanc, T., Querel, R., Tourpali, K., Damadeo, R., Maillard Barras, E., Stübi, R., Vigouroux, C., Arosio, C., Nedoluha, G., Boyd, I., Van Malderen, R., Mahieu, E., Smale, D., Sussmann, R., 2022. Updated trends of the stratospheric ozone vertical distribution in the 60° s–60° n latitude range based on the lotus regression model. *Atmospheric Chemistry and Physics* 22, 11657–11673. URL: <https://acp.copernicus.org/articles/22/11657/2022/>, doi:<https://doi.org/10.5194/acp-22-11657-2022>.
- 195 Godin-Beekmann, S., Porteneuve, J., Garnier, A., 2002. Systematic DIAL lidar monitoring of the stratospheric ozone vertical distribution at Observatoire de Haute-Provence (43.92°N, 5.71°E). *Journal of Environmental Monitoring* 5, 57–67. URL: <https://hal.archives-ouvertes.fr/hal-03326249>, doi:<https://doi.org/10.1039/B205880D>.
- Komhyr, W., 1969. Electrochemical concentration cells for gas analysis. *Annales of Geophysicae* 25, 203–210.
- Komhyr, W.D., Barnes, R.A., Brothers, G.B., Lathrop, J.A., Opperman, D.P., 1995. Electrochemical concentration cell ozonesonde performance evaluation during stoic 1989. *Journal of Geophysical Research: Atmospheres* 100, 9231–9244. URL: <https://agupubs.onlinelibrary.wiley.com/doi/abs/10.1029/94JD02175>, doi:<https://doi.org/https://doi.org/10.1029/94JD02175>, arXiv:<https://agupubs.onlinelibrary.wiley.com/doi/pdf/10.1029/94JD02175>.
- 200 Lin, M., Fiore, A.M., Horowitz, L.W., Langford, A.O., Oltmans, S.J., Tarasick, D., Rieder, H.E., 2015. Climate variability modulates western us ozone air quality in spring via deep stratospheric intrusions. *Nature Communications* 6, 7105–7115. URL: <https://doi.org/10.1038/ncomms8105>, doi:<https://doi.org/10.1038/ncomms8105>.
- 210 Livesey, N., Read, W., Wagner, P., Froidevaux, L., Santee, M., Schwartz, M., Lambert, A., Millán Valle, L., Pumphrey, H., Manney, G., Fuller, R., Jarnot, R., Knosp, B., Lay, R., 2022. Earth observing system (eos) aura microwave limb sounder (mls) version 5.0x level 2 and 3 data quality and description document.
- Nair, P.J., Godin-Beekmann, S., Pazmiño, A., Hauchecorne, A., Ancellet, G., Petropavlovskikh, I., Flynn, L.E., Froidevaux, L., 2011. Coherence of long-term stratospheric ozone vertical distribution time series used for the study of ozone recovery at a northern mid-latitude station. *Atmospheric Chemistry and Physics* 11, 4957–4975. URL: <http://www.atmos-chem-phys.net/11/4957/2011/>, doi:<https://doi.org/10.5194/acp-11-4957-2011>.
- 215 Petropavlovskikh, I., Wild, J.D., Abromitis, K., Effertz, P., Miyagawa, K., Flynn, L.E., Maillard Barras, E., Damadeo, R., McConville, G., Johnson, B., Cullis, P., Godin-Beekmann, S., Ancellet, G., Querel, R., Van Malderen, R., Zawada, D., 2025. Ozone trends in homogenized umkehr, ozonesonde, and coh overpass records. *Atmospheric Chemistry and Physics* 25, 2895–2936. URL: <https://acp.copernicus.org/articles/25/2895/2025/>, doi:<https://doi.org/10.5194/acp-25-2895-2025>.
- 220 Riese, M., Ploeger, F., Rap, A., Vogel, B., Konopka, P., Dameris, M., Forster, P., 2012. Impact of uncertainties in atmospheric mixing on simulated utls composition and related radiative effects. *Journal of Geophysical Research: Atmospheres* 117. URL:



- 225 <https://agupubs.onlinelibrary.wiley.com/doi/abs/10.1029/2012JD017751>, doi:<https://doi.org/https://doi.org/10.1029/2012JD017751>,
arXiv:<https://agupubs.onlinelibrary.wiley.com/doi/pdf/10.1029/2012JD017751>.
- Schwartz, M., Froidevaux, L., Livesey, N., Read, W., Fuller, R., 2020. MLS/Aura Level 3 Daily Binned Ozone (O3) Mixing Ratio on Assorted Grids V004. NASA Goddard Earth Sciences Data and Information Services Center (DAAC) data set, DOI: 10.5067/AURA/MLS/DATA/3117, id.3117 (2020). doi:<https://doi.org/10.5067/AURA/MLS/>.
- 230 Smit, H., Oltmans, S., Deshler, T., Tarasick, D., Johnson, B., Schmidlin, F., Stuebi, R., Davies, J., 2012. SI2N/O3S-DQA activity: Guidelines for homogenization of ozone sonde data, Activity as part of SPARC-IGACO-IOC Assessment (SI2N) "past changes in the vertical distribution of ozone assessment". URL: http://www-das.uwyo.edu/~deshler/NDACC_O3Sondes/O3s_DQA/O3S-DQA-Guidelines%20Homogenization-V2-19November2012.pdf.
- Smit, H., Thompson, A., 2021. GAW report 268 Ozonesonde Measurement Principles and Best Operational Practices: ASOPOS 2.0 (Assessment of Standard Operating Procedures for Ozonesondes). URL: https://library.wmo.int/doc_num.php?explnum_id=10884.
- 235 Steinbrecht, W., Froidevaux, L., Fuller, R., Wang, R., Anderson, J., Roth, C., Bourassa, A., Degenstein, D., Damadeo, R., Zawodny, J., Frith, S., McPeters, R., Bhartia, P., Wild, J., Long, C., Davis, S., Rosenlof, K., Sofieva, V., Walker, K., Rahpoe, N., Rozanov, A., Weber, M., Laeng, A., von Clarmann, T., Stiller, G., Kramarova, N., Godin-Beekmann, S., Leblanc, T., Querel, R., Swart, D., Boyd, I., Hocke, K., Kämpfer, N., Maillard Barras, E., Moreira, L., Nedoluha, G., Vigouroux, C., Blumenstock, T., Schneider, M., García, O., Jones, N., Mahieu, E., Smale, D., Kotkamp, M., Robinson, J., Petropavlovskikh, I., Harris, N., Hassler, B., Hubert, D., Tummon, F., 2017.
- 240 An update on ozone profile trends for the period 2000 to 2016. *Atmospheric Chemistry and Physics* 17, 10675–10690. URL: <https://acp.copernicus.org/articles/17/10675/2017/>, doi:<https://doi.org/10.5194/acp-17-10675-2017>.
- Sterling, C.W., Johnson, B.J., Oltmans, S.J., Smit, H.G.J., Jordan, A.F., Cullis, P.D., Hall, E.G., Thompson, A.M., Witte, J.C., 2018. Homogenizing and estimating the uncertainty in noaa's long-term vertical ozone profile records measured with the electrochemical concentration cell ozonesonde. *Atmospheric Measurement Techniques* 11, 3661–3687. URL: <https://amt.copernicus.org/articles/11/3661/2018/>, doi:<https://doi.org/10.5194/amt-11-3661-2018>.
- 245 Tarasick, D.W., Davies, J., Smit, H.G.J., Oltmans, S.J., 2016. A re-evaluated canadian ozonesonde record: measurements of the vertical distribution of ozone over canada from 1966 to 2013. *Atmospheric Measurement Techniques* 9, 195–214. URL: <https://amt.copernicus.org/articles/9/195/2016/>, doi:<https://doi.org/10.5194/amt-9-195-2016>.
- Van Malderen, R., Allaart, M.A.F., De Backer, H., Smit, H.G.J., De Muer, D., 2016. On instrumental errors and related correction strategies of ozonesondes: possible effect on calculated ozone trends for the nearby sites Uccle and De Bilt. *Atmospheric Measurement Techniques* 9, 3793–3816. URL: <https://amt.copernicus.org/articles/9/3793/2016/>, doi:<https://doi.org/10.5194/amt-9-3793-2016>.
- 250 Van Malderen, R., De Muer, D., De Backer, H., Poyraz, D., Verstraeten, W.W., De Bock, V., Delcloo, A.W., Mangold, A., Laffineur, Q., Allaart, M., Fierens, F., Thouret, V., 2021. Fifty years of balloon-borne ozone profile measurements at Uccle, Belgium: a short history, the scientific relevance, and the achievements in understanding the vertical ozone distribution. *Atmospheric Chemistry and Physics* 21, 12385–12411. URL: <https://acp.copernicus.org/articles/21/12385/2021/>, doi:<https://doi.org/10.5194/acp-21-12385-2021>.
- 255 Wing, R., Steinbrecht, W., Godin-Beekmann, S., McGee, T.J., Sullivan, J.T., Sumnicht, G., Ancellet, G., Hauchecorne, A., Khaykin, S., Keckhut, P., 2020. Intercomparison and evaluation of ground- and satellite-based stratospheric ozone and temperature profiles above Observatoire de Haute-Provence during the Lidar Validation NDACC Experiment (LAVANDE). *Atmospheric Measurement Techniques* 13, 5621–5642. URL: <https://amt.copernicus.org/articles/13/5621/2020/>, doi:<https://doi.org/10.5194/amt-13-5621-2020>.
- 260 Witte, J.C., Thompson, A.M., Smit, H.G.J., Fujiwara, M., Posny, F., Coetzee, G.J.R., Northam, E.T., Johnson, B.J., Sterling, C.W., Mohamad, M., Ogino, S.Y., Jordan, A., da Silva, F.R., 2017. First reprocessing of Southern Hemisphere Additional Ozonesondes (SHADOZ)



- profile records (1998–2015): 1. Methodology and evaluation. *Journal of Geophysical Research: Atmospheres* 122, 6611–6636. URL: <https://agupubs.onlinelibrary.wiley.com/doi/abs/10.1002/2016JD026403>, doi:<https://doi.org/https://doi.org/10.1002/2016JD026403>.
- 265 Witte, J.C., Thompson, A.M., Smit, H.G.J., Vömel, H., Posny, F., Stübi, R., 2018. First Reprocessing of Southern Hemisphere Additional OZonesondes Profile Records: 3. Uncertainty in Ozone Profile and Total Column. *Journal of Geophysical Research: Atmospheres* 123, 3243–3268. URL: <https://agupubs.onlinelibrary.wiley.com/doi/abs/10.1002/2017JD027791>, doi:<https://doi.org/https://doi.org/10.1002/2017JD027791>.
- 270 WMO, 2023. GAW report 278 Scientific Assessment of Ozone Depletion: 2022. Science Report. World Meteorological Organization (WMO) and National Oceanic Atmospheric Administration (NOAA) and National Aeronautics Space Administration (NASA) and European Commission. URL: <https://library.wmo.int/idurl/4/42105>.